# Efficient Co/Pt THz spintronic emitter with tunable polarization ⊘

A. M. Buryakov ✉ (iD) ; A. V. Gorbatova (iD) ; P. Y. Avdeev (iD) ; E. D. Lebedeva (iD) ; K. A. Brekhov (iD) ;
A. V. Ovchinnikov (iD) ; N. S. Gusev; E. A. Karashtin (iD) ; M. V. Sapozhnikov (iD) ; E. D. Mishina (iD) ; N. Tiercelin (iD) ;
V. L. Preobrazhensky (iD)

Check for updates

CrossMark

View
Online

Export
Citation

## Articles You May Be Interested In

A functional integral formalism for quantum spin systems

*J. Math. Phys.* (July 2008)

AIP Publishing

# Efficient Co/Pt THz spintronic emitter with tunable polarization

View Online  Export Citation  CrossMark

A. M. Buryakov,[1,a] [iD] A. V. Gorbatova,[1] [iD] P. Y. Avdeev,[1] [iD] E. D. Lebedeva,[1] [iD] K. A. Brekhov,[1] [iD] A. V. Ovchinnikov,[2] [iD]
N. S. Gusev,[3,4] E. A. Karashtin,[3,4] [iD] M. V. Sapozhnikov,[3,4] [iD] E. D. Mishina,[1] [iD] N. Tiercelin,[5] [iD]
and V. L. Preobrazhensky[6] [iD]

## AFFILIATIONS

[1]MIREA - Russian Technological University, Moscow 119454, Russia
[2]Joint Institute for High Temperatures of the Russian Academy of Sciences, Izhorskaya 13 Bldg. 2, Moscow 125412, Russia
[3]Institute for Physics of Microstructures RAS, Nizhny Novgorod 603950, Russia
[4]Lobachevsky State University, Nizhny Novgorod 603950, Russia
[5]University Lille, CNRS, Centrale Lille, University Polytechnique Hauts-de-France, UMR 8520 -IEMN, 59000 Lille, France
[6]Prokhorov General Physics Institute of RAS, Moscow 119991, Russia

[a]Author to whom correspondence should be addressed: buryakov@mirea.ru

## ABSTRACT

We report on the design of a spintronic emitter based on the Pt(3 nm)/Co(3 nm) structure, which enables the control over terahertz radiation polarization. Utilizing the field-induced magnetization rotation that takes place at low magnetic fields of up to 250 Oe at room temperature, we have achieved the full range of terahertz polarization rotation from 0° to 360°. This rotation became possible due to the uniaxial magnetic anisotropy induced in the plane of the cobalt film during its fabrication. We evaluated the efficiency of the Co/Pt structure in generating terahertz radiation and found that the terahertz pulse energy flux reaches ∼160 nJ/cm² at an excitation flux of 4 mJ/cm².

*Published under an exclusive license by AIP Publishing.* https://doi.org/10.1063/5.0160497

In recent years, advances in terahertz (THz) technologies and magnetism have unveiled the high potential of spintronic THz emitters (STE) based on bilayer structures comprising of magnetic and non-magnetic metal films.[1] Excitation of such structures by femtosecond pulses leads to the generation of subpicosecond spin currents within them, consequently resulting in the emission of broadband terahertz radiation.[2]

One of the key advantages of STE is their ability to control a diverse set of THz radiation parameters (polarization, amplitude, and bandwidth), by applying external magnetic and/or electric fields.[2–4] Such magnetic-field driven solid-state THz sources, with controlled polarization states, show significant promise for the development of functional on-chip devices for THz optospintronics.[4] Optimization of such devices is impossible without a thorough understanding the physical mechanisms and origin of spin dynamics induced by femtosecond radiation.[5–9] Among the most promising applications are ultra-fast data transfer,[2,4,10] next generation wireless communication (6G),[11–13] and ultrafast electromagnetic recording.[14] In addition, THz emitters are simple, easy-to-manufacture structures with high for this type of emitters optical-THz conversion efficiency.

These attributes allow STE to compete with conventional sources of THz radiation, such as photoconductive antennas and inorganic nonlinear optical crystals.[15]

According to the 2023 roadmap,[16] THz spintronics offers not only a unique approach for performing fast spintronic operations but also new functionalities for THz photonics in the field of generation, modulation, and detection of THz radiation. Polarization rotation is one of the functions required in the THz optical schemes. Several works[17–20] have already shown the possibility of THz radiation polarization rotation without mechanical action on the emitter. The proposed emitters possess uniaxial magnetic anisotropy, allowing for magnetic field-induced magnetization rotation and consequently resulting in THz polarization rotation. By applying a magnetic field along the "hard axis," a full 360° rotation of THz radiation polarization has been achieved, as initially demonstrated in Ref. 21. However, the issue of low power output remains a challenge for controllable THz emitters. Currently, the highest energy per pulse achieved at the STE is 90 nJ.[22]

The bilayer films consisting of Co (3 nm) and Pt (3 nm) were deposited by magnetron sputtering on a glass plate (200-$\mu$m thickness)

22 August 2023 15:37:15

in an argon atmosphere at a pressure of $4 \times 10^{-3}$ Torr and room temperature. Prior to deposition, the vacuum chamber was evacuated to $10^{-6}$ Torr. The growth rate is 0.25 nm/s for Pt and 0.125 nm/s for Co. The Si top layer was 5 nm to protect the structure from oxidation. The accuracy in thickness of layer deposition is ~10%. The deposition process was carried out under an applied magnetic field of 400 Oe, aligned in the plane of the samples. Magnetic field assisted fabrication enabled the creation of an easy magnetization axis in the same as magnetic field direction, and facilitated the occurrence of field-induced magnetization rotation. The selection of the thicknesses for the platinum and cobalt layers was guided by the findings of Ref. 22, which demonstrated the maximum optical-terahertz conversion efficiency precisely for these thicknesses.

To measure the parameters of THz generation, including the rotation of the polarization plane, we utilized the conventional method of THz time-domain spectroscopy (THz-TDS).[17,23] A femtosecond laser system, consisting of a Ti:Sapphire laser and a regenerative amplifier (Avesta Project Ltd.), delivered radiation at wavelength of 800 nm, a pulse repetition rate of 3 kHz, and a pulse duration of ~100 fs. The pump beam aperture on the sample surface was about 1 mm. The Co/Pt structure was placed on a nonmagnetic holder between the poles of an electromagnet to control the magnetization. The magnetic field was applied along the X-axis of the laboratory frame in the film plane [Fig. 1(a)]. THz radiation generated by the Co/Pt structure was detected by electro-optical sampling in a setup with a nonlinear optical ZnTe crystal. The polarization of both pump and probe beams was parallel to the [110] axis || Z of the ZnTe crystal. In this geometry, only $E_X$-component of the THz field is detected (see Ref. 23 for details). To determine the polarization of the THz radiation, a wire-grid polarizer (WGP) was installed in front of the ZnTe analyzer.

In order to assess the emitter efficiency, a high-energy chromium-forsterite laser with amplified chirped pulses was employed. This laser system exhibited a pulse duration of 100 fs, a central wavelength of 1240 nm, and a maximum output energy of 20 mJ. It operated at a repetition rate of 10 Hz. The excitation pump beam was collimated to a width of 2.5 cm (FWHM), and the size of the excitation

region on the Co/Pt surface was restricted by a 1.2 cm diameter aperture due to the limited sample size. After the pump pulse passed through the diaphragm, the average fluence ranged from 0.78 to 10 mJ/cm$^2$. Pulse energy was measured using a Golay cell, and the absolute calibration of the spintronic THz emitter was carried out with the setup described in Ref. 24.

The Co/Pt emitters operate on the inverse spin Hall effect (ISHE). The direction of polarization for THz waves emitted due to the ISHE is determined by the directions of the injected spin current and the spin polarization of electrons.[25] The latter depends on the magnetization direction, which is influenced by the magnitude and orientation of the magnetizing field. As a result, the phase of the generated THz waves depends on both the sample orientation relatively to the optical beam and the external magnetic field direction. This dependence is illustrated schematically in Fig. 1(a). Experimental data for THz signals with a pump energy flux of 0.97 mJ/cm$^2$ and two magnetizing field strengths of $+2$ and $-2$ kOe, directed parallel to the easy magnetization axis (E.A.), are shown in Fig. 1(b). These figures depict how the phase of the terahertz wave changes depending on the sample orientation and the applied magnetic field direction. Namely, both a change in the direction of the magnetic field and a change in the orientation of the sample changed the polarity of the terahertz pulse.

Notably, there is a difference in the delay time of terahertz pulses for the two distinct directions of optical beam incidence, "front side" and "back side," as it is seen in Fig. 1(b). This difference is attributed to the optical (n = 1.45[26]) and THz pulses (n ≈ 2.1[27]) delay in the SiO$_2$ substrate, which thickness is 0.18 mm. The decrease in the signal amplitude recorded when irradiating the sample from the Co/Pt film side (front side) can be explained by the high absorption of THz radiation in the glass substrate. Phase flip while changing the geometry from front side to back side confirms the ISHE for THz emission in the studied STE.

Figure 2(a) displays a comparison of temporal profiles of the THz signal for opposite polarities of the magnetic field when samples are irradiated from the substrate side. The phase inversion of the THz signal upon changing the magnetic field direction indicates a 180°
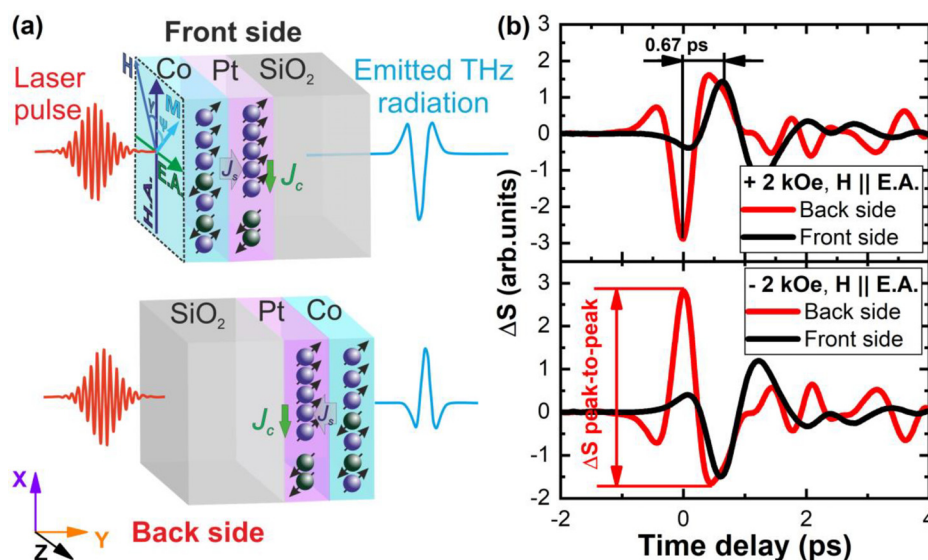
FIG. 1. (a) Schematic representation of the spin current direction and polarity of the generated terahertz waves due to the inverse spin Hall effect; Ψ—angle between magnetic moment and the hard axis, and γ—angle of the magnetic field deflection from the hard axis (b) Time-domain profile of the THz signal ΔS (see supplementary material S.III) for two directions of the optical beam incidence and an applied planar magnetic field of ±2 kOe.
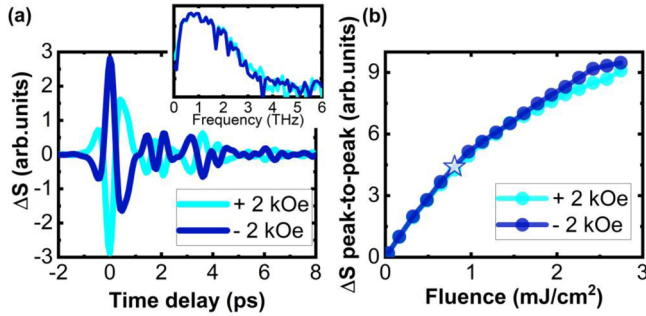
**FIG. 2.** (a) THz polarization rotation resulting from a change in the polarity of the external magnetic field. Inset: Correspondent FTT spectra. (b) Dependence of the THz signal amplitude on the optical radiation energy flux. The star denotes the point corresponding the graph in (a).

rotation of the THz polarization. The inset in Fig. 2(a) presents the spectra of the THz signal. The maximum spectral amplitude is observed at a frequency of 1 THz. The width of the frequency spectrum is limited by 3 THz due to the sensitivity band of the ZnTe detector. Figure 2(b) illustrates the dependence of the THz amplitude on the laser energy flux. The increase in the THz signal with rising pump energy is attributed to the enhanced spin injection from the ferromagnetic layer into the platinum layer.

The dependence of the peak THz amplitude on the applied magnetic field exhibits behavior similar to the standard magnetic hysteresis. Figure 3(a) displays the magnetic hysteresis loops obtained by the THz—TDS method and measured at maximum electric field amplitude, correspondent to the delay time t = 0 ps [see Fig. 2(a)]. Hysteresis loops are presented in two different geometries when the applied magnetic field vector **H** is parallel to the easy magnetization axis (E.A.) or perpendicular to it (H.A.). The shape of the hysteresis loops points to the presence of uniaxial magnetic anisotropy in the sample with an anisotropy field $H_A \approx 120$ Oe. The coercive field of the sample does not exceed 80 Oe.

The presence of magnetic anisotropy with a pronounced hard axis in the Co/Pt sample indicates the possibility of precisely controlled manipulation of the THz polarization by low magnetic fields ($H_A < H < H_A$ up to 120 Oe). To prove that the rotation of THz polarization is the result of a field-induced magnetization rotation induced by an external magnetic field, we studied the angular dependences of the THz signal. In the used optical scheme, polarization rotation angle cannot be seen directly from experimental dependences. The experimental dependences are obtained by fitting them (in Figs. S2 and S3) with the function $\Delta S(t) = \left( f(\phi_2, E_{THz}(\phi_1)) \times \cos(\theta(t)) \right)$.[17,23] In this function, $\theta$ is the phase difference between $\Delta S(t)$ and the reference signal, $t$ represents the delay time,[28] and $f(\phi_2, E_{THz}(\phi_1))$ is the function describing the dependence of the THz electric field,[29] $\phi_2$ is the angle of the WGP polarizer, and $\phi_1$ is the angle between THz field and the [−1,1,0] axis of the ZnTe crystal.

We measured the temporal dependence of the THz signal [Fig. 2(a)] on the rotation angle $\phi_2$ of the WGP polarizer installed in the path of the THz beam. The measurements were made in a magnetic field directed along E.A. or H.A. All measured angular dependences of the THz signal are shown in the supplementary material (Fig. S2 for
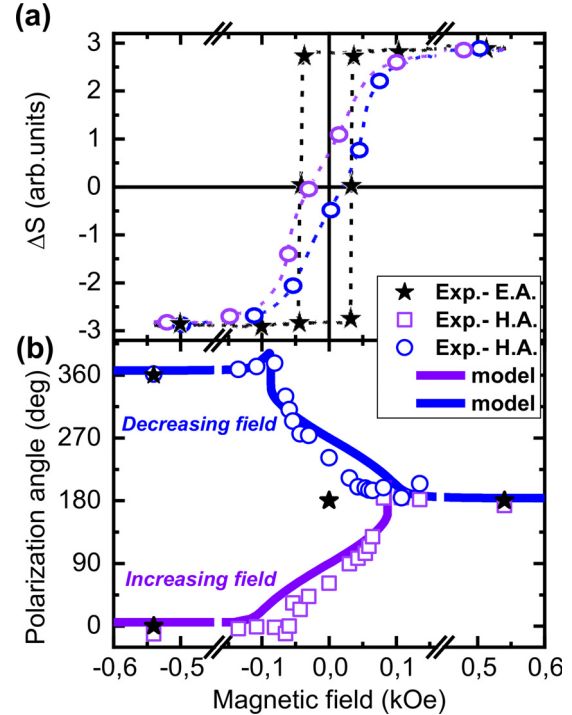


**FIG. 3.** (a) Dependences of THz field amplitude and (b) THz polarization angle on the external magnetic field. The dependence of the THz polarization angle on the magnetic field is obtained from the approximation of angular diagrams (Fig. S2) in the geometry of hard axis and "easy axis" (Fig. S3); The circle and square points are experimental results, while the blue and violet lines represent a model that uses Eq. (1).

the hard axis and Fig. S3 for the easy axis). The extracted from each polarization dependence fitting parameter, angle $\phi_1$ as function of magnetic field is shown in Fig. 3(b). The measurements were carried out with a slight deviation of the magnetizing field from the hard axis (∼1°), which makes it possible for the magnetization vector to fall into one of two opposite directions (see also S3). Otherwise, a domain structure was formed and the effect disappeared.[17,21] Note that, as showed earlier,[17,19] the hysteresis loops for the measured Ex-component of the THz field completely coincide with the hysteresis loops for the magnetization component My. Along with this, the magnetization modulus remains constant, as does the THz field amplitude.

In the framework of ISHE mechanism, the observed rotation of THz polarization is controlled by orientation of the electron spin polarization antiparallel to the magnetic moment of the Co film. The thermodynamic potential $F_m$ of magnetic subsystem of uniaxial magnetic film consist of Zeeman energy of the magnetic moment $\vec{M}$ interaction with the magnetizing field $\vec{H}$ and anisotropy energy characterized by the anisotropy field $H_A$,

$$F_m = -(\vec{M} \cdot \vec{H}) - \frac{H_A}{2M}(\vec{M} \cdot \vec{n})^2, \qquad (1)$$

where $\vec{n}$ is the unit vector parallel to the E.A. axis.

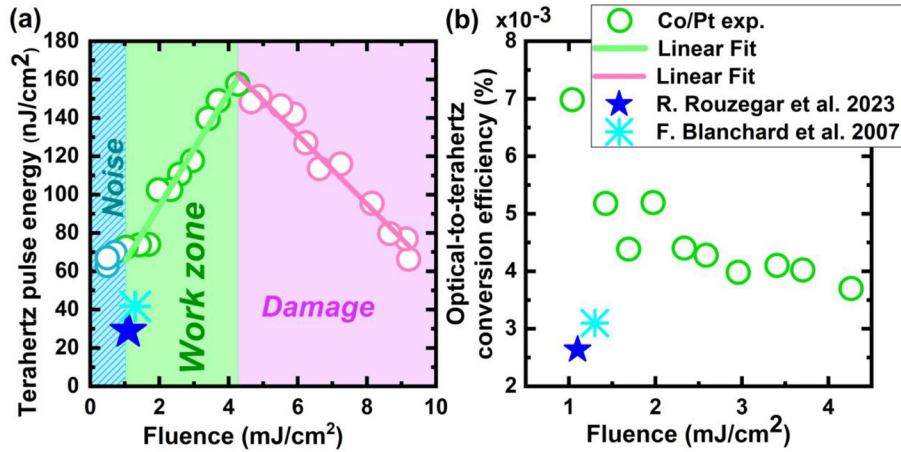The magnetization rotation is described by the equation of state that delivers minimum for $F_m$,

**FIG. 4.** (a) Energy flux of THz radiation from a Co/Pt spintronic emitter in the range of optical pump fluence (1240 nm) 0.78–10 mJ/cm² at a spot size 1.2 cm. The blue star: the maximum THz energy currently achieved in similar STE structures.[22] The cyan asterisk denotes the highest THz energy presently attained in ZnTe crystal as per Refs. 22, 30, and 31. (b) The optical-to-terahertz conversion efficiency.

$$H \cdot \sin(\psi - \gamma) - \frac{1}{2} H_A \cdot \sin 2\psi = 0, \qquad (2)$$

where $\psi$ is the angle between magnetic moment and the hard axis, and $\gamma$ is an angle of the magnetic field deflection from the hard axis [Fig. 1(a)]. We assumed the magnetization value constant ($|\vec{M}|$), in agreement with the Landau theory.

Since the direction of magnetization determines the direction of THz polarization, then Eq. (2) also describes the dependence of the rotation angle $\phi_1$ of the THz polarization on the magnetic field strength (supplementary material II). The result of finding the dependence $\phi_1(H)$ is shown in Fig. 3(b). Solutions of Eq. (1) were found for parameters $H_A = 120$ Oe and $\gamma = 0.03$. The latter was obtained by fitting to experimental data. Near the field-induced magnetization rotation points $H = \pm H_A$, characteristic spikes appear on the calculated curve.

Figure 4(a) shows the generated THz pulse energy density in the range of optical fluence of (1–10) mJ/cm². The minimum detected THz pulse energy density was about 70 nJ/cm² at the optical pump fluence of 1.5 mJ/cm². For lower fluences, the THz energy remained on the noise level. In the range of 1–4 mJ/cm², the THz pulse energy increased linearly and reached the highest value of 160 nJ/cm². For the pump fluence above the threshold value of 4.2 mJ/cm², the THz pulse energy decreased irreversibly (this area is marked as "Damage" in Fig. 4). Enhancing thermal conductivity with a silicon substrate[22] might enable increasing this threshold.

Figure 4(b) demonstrates the efficiency of the optical-to-THz conversion in the range of optical fluence of (1–4.5) mJ/cm². The maximal THz emission efficiency from a spintronic emitter was reported in Ref. 22. The peak THz pulse energy was 29 nJ/cm² with an excitation beam width of 2 cm (full width at half maximum, FWHM, of intensity) and a maximum fluence of 1.1 mJ/cm². At the maximum pump energy of 48 mJ (1.33 mJ/cm²) for the nonlinear ZnTe crystal, the THz pulse energy amounts to 1.5 μJ (or, when normalized to the excitation area, 41.67 nJ/cm²).[30] In comparison with that work and normalizing by the effective generation area (the pump beam width), we achieved 2.4-fold increase in the efficiency at the optical pump fluence of 1.1 mJ/cm² and 5.5-fold increase at the fluence of 4 mJ/cm². The spintronic emitter demonstrated an optical-to-terahertz conversion of $7 \times 10^{-3}$%. In previous studies, values of $2.6 \times 10^{-3}$% for the

spintronic emitter and $3.1 \times 10^{-3}$% for the nonlinear ZnTe crystal were achieved.[31]

In summary, this research highlights the potential for controlled manipulation of THz polarization in a Co/Pt spintronic emitter by applying an external magnetic field. By rotating magnetization within field-induced magnetization rotation by changing magnetizing field value only, the rotation angle of the THz polarization can be controlled by 360°. Studies of the dependences of the peak THz amplitude and the polarization angle on the applied magnetic field yielded results consistent with the theoretical model based on the equation of state for uniaxial magnetic films. Additionally, a linear correlation was observed between terahertz pulse energy and excitation pump intensity for the Co/Pt spintronic emitter. The THz generator achieved its highest pulse energy flux of ∼160 nJ/cm² at the optical pump fluence of about 4 mJ/cm². This was achieved by combination of the most efficient STE structure (Co/Pt) with the creation of uniaxial magnetic anisotropy in it, accompanied by field-induced magnetization rotation. In-plane field-induced magnetization rotation is the tool for rotation of THz polarization.

This study offers valuable insight into manipulating THz polarization in spintronic emitters, opening up potential applications in fields, such as communication, imaging, and sensing. By employing advanced materials and enhancing thermal conductivity with a silicon substrate, further improvements in emitter performance and thermal stability may be realized.

See the supplementary material for an in-depth examination of the angular dependences derived from terahertz time domain spectroscopy, the findings of which were utilized in the construction of Fig. 3(b). This material presents results depicting the relationship between the intensity of terahertz generation and the polarization angle of the optical pump beam. Additionally, it elucidates the process behind calculating the detected X-component of the terahertz field. A comprehensive discussion regarding the 360° rotation of the magnetization, achieved via two jumps in fields marginally smaller than the critical field $H_A$, is also included.

emitters were designed and fabricated using the facilities of the Center of Excellence "Center of Photonics" and funded by The Ministry of Science and Higher Education (Contract No. 075-15-2022-316).

## AUTHOR DECLARATIONS
### Conflict of Interest

The authors have no conflicts to disclose.

### Author Contributions

**Arseniy Buryakov:** Conceptualization (equal); Writing – original draft (equal). **Elena D. Mishina:** Writing – review & editing (equal). **Nicolas Tiercelin:** Conceptualization (equal). **Vladimir Preobrazhensky:** Conceptualization (equal); Writing – review & editing (equal). **Anastasiya V. Gorbatova:** Data curation (equal). **Pavel Y. Avdeev:** Methodology (equal). **Ekaterina D. Lebedeva:** Software (equal). **Kirill A. Brekhov:** Formal analysis (equal). **Andrey V. Ovchinnikov:** Data curation (equal). **Nikita S. Gusev:** Methodology (equal). **Evgeny Karashtin:** Formal analysis (equal). **Maksim V. Sapozhnikov:** Project administration (equal).

## DATA AVAILABILITY

The data that support the findings of this study are available from the corresponding author upon reasonable request.

## REFERENCES

[1]T. Seifert, S. Jaiswal, U. Martens, J. Hannegan, L. Braun, P. Maldonado, F. Freimuth, A. Kronenberg, J. Henrizi, I. Radu, E. Beaurepaire, Y. Mokrousov, P. M. Oppeneer, M. Jourdan, G. Jakob, D. Turchinovich, L. M. Hayden, M. Wolf, M. Münzenberg, M. Kläui, and T. Kampfrath, "Efficient metallic spintronic emitters of ultrabroadband terahertz radiation," Nat. Photonics **10**(7), 483–488 (2016).

[2]X. Chen, X. Wu, S. Shan, F. Guo, D. Kong, C. Wang, T. Nie, C. Pandey, L. Wen, W. Zhao, C. Ruan, J. Miao, Y. Li, and L. Wang, "Generation and manipulation of chiral broadband terahertz waves from cascade spintronic terahertz emitters," Appl. Phys. Lett. **115**(22), 221104 (2019).

[3]P. Li, S. Liu, X. Chen, C. Geng, and X. Wu, "Spintronic terahertz emission with manipulated polarization (STEMP)," Front. Optoelectron. **15**(1), 12 (2022).

[4]D. Kong, X. Wu, B. Wang, T. Nie, M. Xiao, C. Pandey, Y. Gao, L. Wen, W. Zhao, C. Ruan, J. Miao, Y. Li, and L. Wang, "Broadband spintronic terahertz emitter with magnetic-field manipulated polarizations," Adv. Opt. Mater. **7**(20), 1900487 (2019).

[5]V. Unikandanunni, R. Medapalli, M. Asa, E. Albisetti, D. Petti, R. Bertacco, E. E. Fullerton, and S. Bonetti, "Inertial spin dynamics in epitaxial cobalt films," Phys. Rev. Lett. **129**(23), 237201 (2022).

[6]S. Gang, R. Adam, M. Plötzing, M. von Witzleben, C. Weier, U. Parlak, D. E. Bürgler, C. M. Schneider, J. Rusz, P. Maldonado, and P. M. Oppeneer, "Element-selective investigation of femtosecond spin dynamics in NiPd magnetic alloys using extreme ultraviolet radiation," Phys. Rev. B **97**(6), 064412 (2018).

[7]V. Unikandanunni, R. Medapalli, E. E. Fullerton, K. Carva, P. M. Oppeneer, and S. Bonetti, "Anisotropic ultrafast spin dynamics in epitaxial cobalt," Appl. Phys. Lett. **118**(23), 232404 (2021).

[8]D. Rudolf, C. La-O-Vorakiat, M. Battiato, R. Adam, J. M. Shaw, E. Turgut, P. Maldonado, S. Mathias, P. Grychtol, H. T. Nembach, T. J. Silva, M. Aeschlimann, H. C. Kapteyn, M. M. Murnane, C. M. Schneider, and P. M. Oppeneer, "Ultrafast magnetization enhancement in metallic multilayers driven by superdiffusive spin current," Nat. Commun. **3**(1), 1037 (2012).

[9]R. Medapalli, G. Li, S. K. K. Patel, R. V. Mikhaylovskiy, T. Rasing, A. V. Kimel, and E. E. Fullerton, "Femtosecond photocurrents at the FeRh/Pt interface," Appl. Phys. Lett. **117**(14), 142406 (2020).

[10]W. Withayachumnankul, M. Fujita, and T. Nagatsuma, "Integrated silicon photonic crystals toward terahertz communications," Adv. Opt. Mater. **6**(16), 1800401 (2018).

[11]W. Deng, L. Chen, H. Zhang, S. Wang, Z. Lu, S. Liu, Z. Yang, Z. Wang, S. Yuan, Y. Wang, R. Wang, Y. Yu, X. Wu, X. Yu, and X. Zhang, "On-chip polarization- and frequency-division demultiplexing for multidimensional terahertz communication," Laser Photonics Rev. **16**(10), 2200136 (2022).

[12]C. Zhang, G. Zhou, J. Wu, Y. Tang, Q. Wen, S. Li, J. Han, B. Jin, J. Chen, and P. Wu, "Active control of terahertz waves using vanadium-dioxide-embedded metamaterials," Phys. Rev. Appl. **11**(5), 054016 (2019).

[13]Y. Yang, Y. Yamagami, X. Yu, P. Pitchappa, J. Webber, B. Zhang, M. Fujita, T. Nagatsuma, and R. Singh, "Terahertz topological photonics for on-chip communication," Nat. Photonics **14**(7), 446–451 (2020).

[14]A. V. Kimel and M. Li, "Writing magnetic memory with ultrashort light pulses," Nat. Rev. Mater. **4**(3), 189–200 (2019).

[15]L. Cheng, Z. Li, D. Zhao, and E. E. M. Chia, "Studying spin–charge conversion using terahertz pulses," APL Mater. **9**(7), 070902 (2021).

[16]A. Leitenstorfer, A. S. Moskalenko, T. Kampfrath, J. Kono, E. Castro-Camus, K. Peng, N. Qureshi, D. Turchinovich, K. Tanaka, A. G. Markelz, M. Havenith, C. Hough, H. J. Joyce, W. J. Padilla, B. Zhou, K.-Y. Kim, X.-C. Zhang, P. U. Jepsen, S. Dhillon, M. Vitiello, E. Linfield, A. G. Davies, M. C. Hoffmann, R. Lewis, M. Tonouchi, P. Klarskov, T. S. Seifert, Y. A. Gerasimenko, D. Mihailovic, R. Huber, J. L. Boland, O. Mitrofanov, P. Dean, B. N. Ellison, P. G. Huggard, S. P. Rea, C. Walker, D. T. Leisawitz, J. R. Gao, C. Li, Q. Chen, G. Valušis, V. P. Wallace, E. Pickwell-MacPherson, X. Shang, J. Hesler, N. Ridler, C. C. Renaud, I. Kallfass, T. Nagatsuma, J. A. Zeitler, D. Arnone, M. B. Johnston, and J. Cunningham, "The 2023 terahertz science and technology roadmap," J. Phys. D: Appl. Phys. **56**(22), 223001 (2023).

[17]D. Khusyainov, S. Ovcharenko, M. Gaponov, A. Buryakov, A. Klimov, N. Tiercelin, P. Pernod, V. Nozdrin, E. Mishina, A. Sigov, and V. Preobrazhensky, "Polarization control of THz emission using spin-reorientation transition in spintronic heterostructure," Sci. Rep. **11**(1), 697 (2021).

[18]D. Khusyainov, S. Ovcharenko, A. Buryakov, A. Klimov, P. Pernod, V. Nozdrin, E. Mishina, A. Sigov, V. Preobrazhensky, and N. Tiercelin, "Composite multiferroic terahertz emitter: Polarization control via an electric field," Phys. Rev. Appl. **17**(4), 044025 (2022).

[19]S. M. Hewett, C. Bull, A. M. Shorrock, C.-H. Lin, R. Ji, M. T. Hibberd, T. Thomson, P. W. Nutter, and D. M. Graham, "Spintronic terahertz emitters exploiting uniaxial magnetic anisotropy for field-free emission and polarization control," Appl. Phys. Lett. **120**(12), 122401 (2022).

[20]P. Agarwal, L. Huang, S. Ter Lim, and R. Singh, "Electric-field control of non-linear THz spintronic emitters," Nat. Commun. **13**(1), 4072 (2022).

[21]P. Koleják, G. Lezier, K. Postava, J.-F. Lampin, N. Tiercelin, and M. Vanwolleghem, "360° polarization control of terahertz spintronic emitters using uniaxial FeCo/TbCo₂/FeCo trilayers," ACS Photonics **9**(4), 1274–1285 (2022).

[22]R. Rouzegar, A. L. Chekhov, Y. Behovits, B. R. Serrano, M. A. Syskaki, C. H. Lambert, D. Engel, U. Martens, M. Münzenberg, M. Wolf, G. Jakob, M. Kläui, T. S. Seifert, and T. Kampfrath, "Broadband spintronic terahertz source with peak electric fields exceeding 1.5 MV/cm," Phys. Rev. Appl. **19**(3), 034018 (2023).

[23]F. A. Zainullin, D. I. Khusyainov, M. V. Kozintseva, and A. M. Buryakov, "Polarization analysis of THz radiation using a wire grid polarizer and ZnTe crystal," Russ. Tech. J. **10**(3), 74–84 (2022).

[24]C. Vicario, A. V. Ovchinnikov, S. I. Ashitkov, M. B. Agranat, V. E. Fortov, and C. P. Hauri, "Generation of 09-mJ THz pulses in DSTMS pumped by a Cr:Mg₂SiO₄ laser," Opt. Lett. **39**(23), 6632 (2014).

[25]T. S. Seifert, "Spintronics with terahertz radiation: Probing and driving spins at highest frequencies," Ph.D. dissertation (Freien Universität Berlin, Berlin, 2017).

[26]Y. Arosa and R. de la Fuente, "Refractive index spectroscopy and material dispersion in fused silica glass," Opt. Lett. **45**(15), 4268 (2020).

[27]C. L. Davies, J. B. Patel, C. Q. Xia, L. M. Herz, and M. B. Johnston, "Temperature-dependent refractive index of quartz at terahertz frequencies," J. Infrared, Millim. THz Waves **39**(12), 1236–1248 (2018).

[28]Z. Jiang, F. G. Sun, Q. Chen, and X.-C. Zhang, "Electro-optic sampling near zero optical transmission point," Appl. Phys. Lett. **74**(9), 1191–1193 (1999).

[29]M. Brunken, H. Genz, P. Göttlicher, C. Hessler, M. Hüning, H. Loos, A. Richter, H. Schlarb, P. Schmüser, S. Simrock, and D. Suetterlin, "Electro-optic sampling at the TESLA test accelerator: Experimental setup and first results," TESLA Report 11, 2003.

[30]F. Blanchard, L. Razzari, H. C. Bandulet, G. Sharma, R. Morandotti, J. C. Kieffer, T. Ozaki, M. Reid, H. F. Tiedje, H. K. Haugen, and F. A. Hegmann, "Generation of 1.5 $\mu$J single-cycle terahertz pulses by optical rectification from a large aperture ZnTe crystal," Opt. Express **15**(20), 13212 (2007).

[31]See https://www.swissterahertz.com/oh1 for "Swiss Terahertz."

22 August 2023 15:37:15